

Original Research

Astaxanthin suppresses cigarette smoke and lipopolysaccharide-induced airway inflammation through induction of heme oxygenase-1

Liu Nian¹, Zhang Weidong¹, Luo Shujuan², Cao Jun¹, Peng Minlian¹, Liu Zhiguang^{1*}¹ Department of Respiration, Hunan Provincial People's Hospital and The First Affiliated Hospital of Hunan Normal University, Changsha, Hunan 410005, China² Department 1 of Respiration, Hunan Children's Hospital, Changsha, Hunan 410007, China

Correspondence to: fg1308@163.com

Received October 23, 2018; Accepted January 29, 2019; Published January 31, 2019

Doi: <http://dx.doi.org/10.14715/cmb/2019.65.1.17>

Copyright: © 2019 by the C.M.B. Association. All rights reserved.

Abstract: The present study was carried out to evolve an effective treatment strategy for chronic obstructive pulmonary disease (COPD). Astaxanthin (AS) is abundantly present in red pigments of crustaceans, and has also been proven to have considerable biological activities. The anti-inflammatory effect of AS was evaluated in lipopolysaccharide (LPS)-exposed RAW264.7 macrophages. It was found that AS markedly inhibited elevation of NO and pro-inflammatory mediators. Moreover, it downregulated iNOS in LPS-stimulated RAW264.7 cells, suppressed the release of pro-inflammatory cytokines, and decreased ROS levels in mice exposed to cigarette smoke (CS) and LPS. These results imply that AS has therapeutic and prophylactic potential in the airway inflammatory response associated with COPD.

Key words:

Introduction

Recent decades have witnessed rising cases of chronic inflammatory respiratory ailments such as COPD and asthma. Indeed, it has been projected that COPD may rank third in the list of killer diseases by 2020 (1, 2). Although the pathogenesis of COPD is multi-factorial, CS is thought to be one of the main pre-disposing agents (3). For instance, CS induces the recruitment of macrophages and neutrophils through the release of pro-inflammatory cytokines and chemo-attractants (4, 5). Neutrophil influx is the main pathophysiological characteristic of COPD. Continuous activation of neutrophils increases the release of ROS, inflammation-linked cytokines, and tissue lysate containing matrix metalloproteinases and elastases (6, 7). These aggravate airway inflammation and induction of destruction of the normal alveolar structure. Macrophages affect airway inflammatory cells by producing inflammatory cytokines and chemokines during the pathogenesis of COPD (8). Thus, the inhibition of production of these cytokines and chemokines is considered very essential in the control of respiratory diseases. Although current medical treatments can ease the symptoms of the disease, and numerous research have resulted in production of many therapeutic agents (9, 10), current research efforts are concentrated on new drugs with enhanced potency in ameliorating the symptoms of these diseases (11).

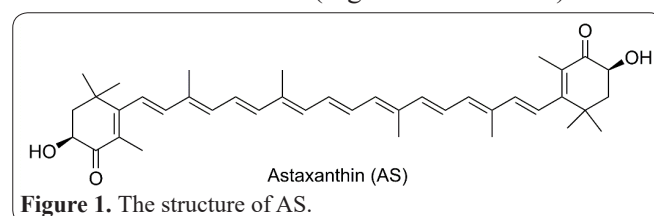
The structure of AS (3, 3'-dihydroxy- β , β' -carotene-4,4'-dione) is shown in Figure 1. It is a non-provitamin A carotene-like compound categorized as xanthophyll, which is present in high amounts in red pigments of

crustaceans (crabs and shrimps), squid, and asteroidean (12). Studies have demonstrated that AS has beneficial pharmacological properties such as antioxidant (100 - 550 times more active than vitamin E), anti-cancer, NO-scavenging and anti-inflammatory effects (13, 14). Based on the biological characteristic of this naturally-occurring carotenoid, it can also be used as a vascular endothelial protective agent. Recent researches in animal models of diabetes and hypertension have indicated that AS lessens endothelial dysfunction underlying vascular endothelial lesions. Notwithstanding the beneficial effects of AS, no studies have been carried out on its suitability for use in the treatment of CS-induced COPD. Therefore, it was theorized, as a basis of the current study, that AS may be effective in reducing COPD inflammation caused by CS. To ascertain this, the anti-inflammatory effects of AS were determined *in vitro*, and *in vivo* in mice exposed to CS and LPS, with a view to determining its potential for use in managing COPD.

Materials and Methods

Materials and reagents

AS was bought from J&K Scientific (Beijing, China) and solubilised in DMSO (Sigma Chemical Co) as stock





solution. Roflumilast (ROF) and MTT were purchased from Sigma Chemical Co. (USA). Antibodies against β -actin, iNOS, p-Nrf2, Nrf2 and HO-1 were products of Santa Cruz Biotech (USA).

Cell culture

The RAW264.7 macrophages (ATCC, VA, USA) were cultured at 37°C in DMEM containing 10% fetal bovine serum (FBS), and 100 units/mL each of penicillin and streptomycin (Invitrogen, USA) in a humidified atmosphere with 5% CO₂.

Determination of cytotoxicity of AS

The cytotoxicity of AS to RAW264.7 cells was determined using MTT assay. The cells (2×10^5 cells/mL) were cultured in a 96-well for 24 h, and then exposed separately to graded levels of AS (10, 20, 40, 60, 80, and 100 M) for 48 h. Thereafter, MTT (0.5 mg/mL, 20 mL) was added to each culture well and the cells were continuously incubated at the temperature of 37 °C for 4 h. After removing the MTT, the formazan crystals formed were solubilized in DMSO (200 μ L) for 10 min, and the absorbance of the solution was read at 540 nm in a microplate reader (Infinite F200 Pro, Tecan, Switzerland). The absorbance values were used as index of cell viability, relative to absorbance for cells incubated in control medium which were considered to be 100 % viable.

Assay of nitric oxide (NO) levels

The RAW264.7 cells were cultured exactly in the same manner, for the same period and at the same density as outlined in the cytotoxicity assay. Thereafter, the cells were incubated for 1 h with AS at concentrations of 5, 10 and 20 μ M, and then stimulated for 16 h with 1 μ g/mL LPS (Sigma-Aldrich). Then, culture supernatant (100 μ L) was added to 100 μ L of Griess reagent in a 96-well plate. The resultant solution was incubated at room temperature for 15 min, and absorbance was read at 540 nm. The NO was extrapolated from a sodium nitrite standard calibration curve. The results were expressed as mean \pm SD of four replicates.

Western blotting

The RAW264.7 cells (2×10^5 cells/mL) were cultured for 24 h, and pretreated with AS at concentrations of 10 and 20 μ M. After incubation for 1 h, they were subjected to stimulation with LPS (1 g/mL). After 6 h, Nrf2 activation was assayed in the cells and in lung tissues excised after 6 h of AS exposure. The expression of HO-1 was determined 24 h after AS exposure. The cells were harvested, lysed for 30 min with lysis buffer containing a protease inhibitor, and centrifuged. The lung tissues were extracted with 1:10 (w: v) mixture of lysis buffer and extracting solution containing protease inhibitor. The total protein content of the lysate was assayed, and equal amounts of protein were separated using SDS-polyacrylamide gel electrophoresis. The resultant bands were transferred onto nitrocellulose membranes and incubated with 1:1000 dilutions of rabbit polyclonal antibodies (iNOS, Nrf2, p-Nrf2, HO-1, and anti- β -actin). Non-specific binding was blocked with 5% skimmed milk. The membranes were rinsed in TBST at room temperature and incubated for 2 h

with a 1:2000 dilution of Peroxidase-AffiniPure goat anti-rabbit IgG (H+L) and Peroxidase-AffiniPure goat anti-mouse IgG (H+L). After washing with TBST, the membranes were subjected to chemiluminescence using Thermo Fisher Chemiluminescence kits. The bands were visualized with an LAS-4000 image analyzer and subjected to densitometric analysis using Fuji Multin Gauge software.

Assay of IL-6, IL-1 β and TNF- α

The cell supernatant levels of TNF- α , IL-6, and IL-1 β were assayed with ELISA kits from R&D Systems in strict compliance with the kit protocol.

Preparation of mouse model of CS and LPS-induced airway inflammation, and mice groupings

Male, 6-week-old C57BL/6N mice were used after a 7-day acclimatization to laboratory conditions in an environment free from specific pathogens. The mice were randomly assigned to four groups (7 mice/group) viz: normal control (NC) group, CS + LPS group, 10 mg/kg roflumilast (ROF, positive control) group, and AS group (administered 10 and 20 mg / kg AS). The CS exposure was carried out as follows: the entire bodies of the mice were exposed for 1 h daily for 10 days to either indoor air or CS from 8 sticks of cigarettes. The CS was produced from 3R4F study cigarettes containing (per stick) 11.0 mg total particulate matter, 9.4 mg tar and 0.76 mg nicotine. The ROF and AS were dissolved in phosphate buffered saline (PBS) containing 1% DMSO + 1% Tween-20, and administered daily orally for 9 days. One hour after the final ROF and AS treatment, mice were intra-nasally administered LPS (μ g in 30 μ L of distilled water). The study protocol was in line with the guidelines of local Institutional Animal Care and Use Committee, and was carried out according to the National Institute of Health guidelines for the care and use of laboratory animals and the National Animal Welfare Act.

Assay pro-inflammatory cytokines and ROS

In line with previously described procedure (15), intracellular ROS levels were assayed using 2',7'-dichlorofluorescein diacetate (DCF-DA) obtained from Sigma-Aldrich, USA. Following rinsing in PBS, the BALF cells were subjected to incubation at 37 °C for 10 min with 20 μ M DCF-DA, and thereafter their ROS contents were measured in a fluorescent plate reader at wavelength of 488 nm and emission fluorescence wavelength of 525 nm. The levels of pro-inflammatory cytokines were determined with R&D ELISA kits, and absorbance was read in a microplate reader at 450 nm.

Real-time polymerase chain reaction (PCR) analysis

The lung tissues of model mice were extracted with 1:10 (w: v) mixture of lysis buffer to measure the mRNA expression of Nrf2, p-Nrf2 and HO-1. Total mRNA was extracted and reverse transcribed, then detected by quantitative real-time PCR using the iCycler real-time detection system (Bio-Rad, USA) in a two-step method. The hot start enzyme was activated at 95°C for 5 min. Subsequently, cDNA was amplified for 40 cycles, which consisted of denaturation at 95°C for 15s and annealing/extension at 58°C for 30s. A melt curve analysis was then performed (the temperature was 55°C for 1 min and

then increased by 0.5°C every 10 s) to detect the formation of primer-derived trimmers and dimers. The primer sequences used were the following: Nrf2 forward, 5'-CGGTATGCAACAGGACATTG-3', and reverse, 5'-ACTGGTTGGGGTCTTCTGTG-3'; p-Nrf2 forward, 5'-TGGACGGGACTATTGAAGGCT-3', and reverse, 5'-GCGGATTGACCGTAATGGGATA-3'; HO-1 forward, 5'-AAGATTGCCAGAAAGCCC-TGGAC-3', and reverse, 5'-AACTGTCGCCACCA-GAAAGCTGAG-3' and β -actin forward, 5'-GTGG-GCGCCCCAGACACCA-3', and reverse, 5'-CTCCT-TAATGTCACGCACGATTC-3'. β -actin was used as internal control.

Statistical analysis

Results were presented as mean \pm standard deviation (SD), and were statistically analyzed using Student's *t*-test. Values of $p < 0.05$ were assumed to indicate statistical significance.

Results

Effect of AS on cell cytotoxicity in RAW264.7 cells

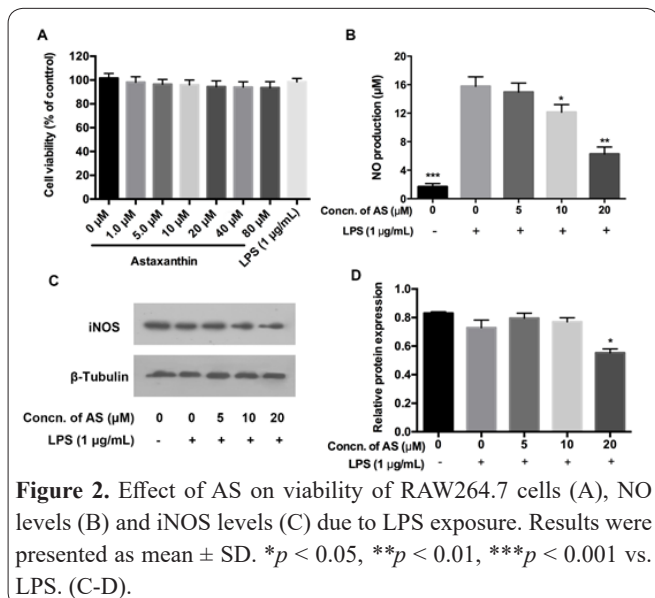
Different doses of AS were co-incubated for 48 h with RAW264.7 cells, and cell viability was assessed with MTT assay. In Figure 2A, even at concentrations up to 80 μ M, AS was not cytotoxic to the RAW264.7 cells. Therefore, AS at non-toxic concentration was chosen for potent anti-inflammatory assays in the subsequent assays.

Effects of AS on NO and the expression of iNOS as a function of LPS stimulation

Compared to untreated cells, LPS-stimulated cells showed a substantial rise in NO production. However, AS significantly reduced the NO production in a dose-dependent manner, when compared to LPS-stimulated cells (Fig. 2B). Besides, AS treatment inhibited iNOS expression caused by LPS treatment in a dose-dependent manner (Fig. 2C-D).

Effects of AS on TNF- α , IL-6, and IL-1 β production in LPS-stimulated RAW264.7 cells

As shown in Fig. 3, when compared to untreated



cells, LPS-exposed cells showed increased IL-6 levels. However, AS treatment significantly and dose-dependently decreased the LPS-induced increases in IL-6 levels, when compared with the LPS-exposed cells (Fig. 3A). In contrast to the results for IL-6, the LPS-stimulated cells had significant increases in TNF- α and IL-1 β , relative to untreated cells, but these increases were reversed by AS (Fig. 3B and Fig. 3C).

Effects of AS on mice model of CS and LPS-induced airway inflammation

Increases in the amount of macrophages and neutrophils are fundamental features of CS- and LPS-induced airway inflammation. Thus, the effect of AS on these cell infiltrations were evaluated with Diff-Quik staining. The results shown in Figures 4A-4B indicate significant and dose-dependent increases in the populations of macrophages and neutrophils in the CS + LPS group, while there were significant and dose-dependent decreases in the number of these cells in the AS group.

Effect of AS on ROS and pro-inflammatory cytokines

Intranasal administration of LPS, and CS exposure significantly increased the levels of TNF- α , IL-6 and ROS. However, treatment with AS led to significant and dose-dependent reductions in the levels of these parameters (Figures 5A-5C). The effects produced by 20 mg/kg AS and 10 mg/kg ROF were comparable.

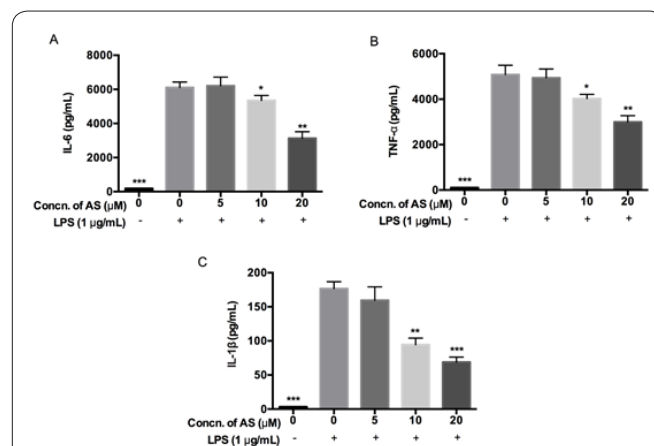


Figure 3. Effect of AS on TNF- α (A), IL-6 (B), and IL-1 β (C) levels in LPS-exposed RAW264.7 cells. Results were presented as mean \pm SD. * $p < 0.05$, ** $p < 0.01$, *** $p < 0.001$, compared to LPS.

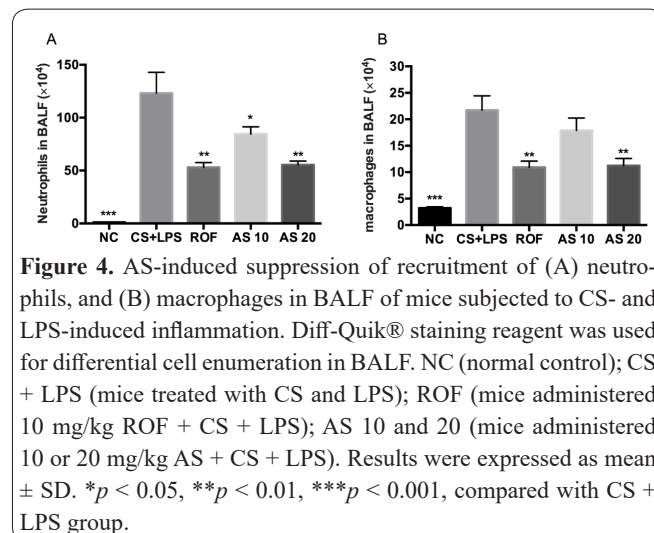


Figure 4. AS-induced suppression of recruitment of (A) neutrophils, and (B) macrophages in BALF of mice subjected to CS- and LPS-induced inflammation. Diff-Quik® staining reagent was used for differential cell enumeration in BALF. NC (normal control); CS + LPS (mice treated with CS and LPS); ROF (mice administered 10 mg/kg ROF + CS + LPS); AS 10 and 20 (mice administered 10 or 20 mg/kg AS + CS + LPS). Results were expressed as mean \pm SD. * $p < 0.05$, ** $p < 0.01$, *** $p < 0.001$, compared with CS + LPS group.

Effect of AS on the expression of HO-1 in the lungs

There was an increase in HO-1 expression in the AS group, relative to the NC or ROF groups (Fig. 6A). Activation of Nrf2, which is a major transcription factor of HO-1, was also observed following AS administration and HO-1 production (Fig. 6B).

Effect of AS on the expression of mRNA level by Real-Time PCR

There was a remarkable decrease in mRNA of HO-1 and Nrf2 expression in the AS group, relative to ROF group (Fig. 7A-B).

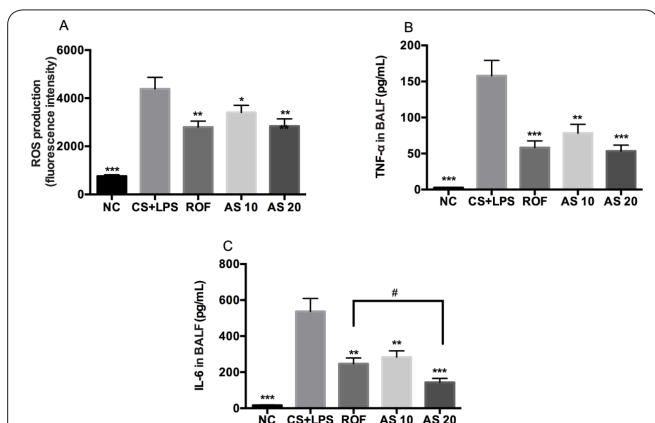


Figure 5. Effect of AS on ROS, TNF- α and IL-6 in BALF CS and LPS-exposed mice. Results were presented as mean \pm SD. ** p < 0.01, *** p < 0.001, relative to CS + LPS group; # p < 0.05, compared to ROF group.

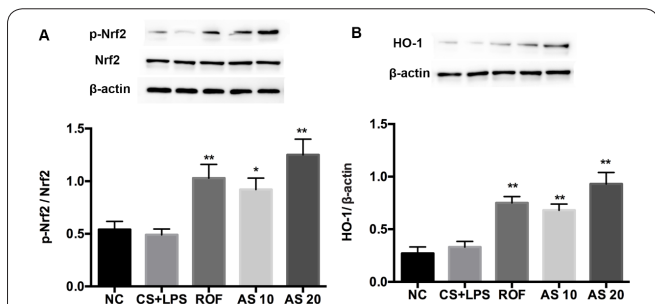


Figure 6. Effect of AS on HO-1 expression in lung tissues of CS-LPS-treated mice. (A) Nrf2 activation, and (B) HO-1 expression. Results were presented as mean \pm SD; * p < 0.05, ** p < 0.01, relative to CS + LPS group.

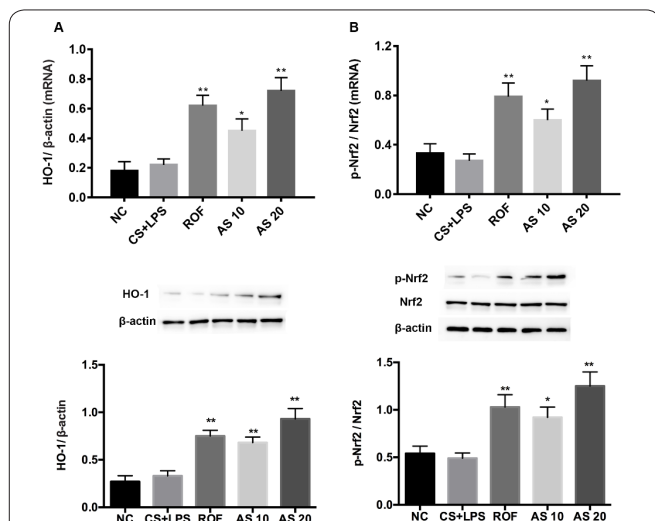


Figure 7. Effect of AS on the expression of mRNA level by Real-Time PCR. (A) HO-1 expression, and (B) Nrf2 activation. Results were presented as mean \pm SD; * p < 0.05, ** p < 0.01, relative to CS + LPS group.

Discussion

The major features of COPD are increases in airway and lung parenchyma levels of macrophages, inflammation markers, neutrophils, macrophages, and inflammatory mediators (16). In view of the importance of airway inflammation in COPD (17), the protective effect of AS was investigated in a CS- and LPS-induced mouse model of airway inflammation. The results showed that AS suppressed recruitment of inflammatory mediators by reducing ROS production and pro-inflammatory mediators in CS- and LPS-exposed mice. Consistent with results obtained *in vivo*, AS suppressed increases in iNOS levels as well as levels of NO and pro-inflammatory mediators in LPS-stimulated RAW264.7 cells. The pathogenesis of COPD is linked to pro-inflammatory cytokines, chemokines, ROS and tissue lyase, all of which lead to airway inflammation (18). The recognition of neutrophils is linked to ROS and cytokines which result in release of TNF- α , IL-1 β and IL-6 (19). Studies have shown that ROS exacerbate airway inflammation by stimulating specific inflammatory signals such as NF- κ B and MAPK (20). CS is an effective stimulant for the release of inflammatory cells into the respiratory tract (21). Previous researches have established that CS enhances neutrophils recruitment into the airways by increasing ROS production (22). In the present study, the effect produced by 20 mg/kg AS in mice were comparable to those produced in mice treated with ROF. This result suggested that AS could efficiently inhibit the CS- and LPS-induced recruitment of inflammatory cells into the airways.

It has been demonstrated that IL-6, TNF- α , and IL-1 β participate in the response to inflammation by stimulating the activating inflammatory signals close to lesion areas (23). Therefore, the inhibition of expressions of pro-inflammatory cytokines can be thought as a vital step towards controlling inflammatory responses. In this study, CS and LPS exposure provoked significant increase in BALF protein content through elevations in IL-6, TNF- α and IL-1 β . However, AS reversed the CS- and LPS-induced increases in BALF cytokines. The results from *in vivo* studies were in agreement with those obtained *in vitro* in support of the anti-inflammatory effects of AS.

The production of NO is strongly associated with the inflammatory process. Nitric oxide (NO) is synthesized from L-arginine in a reaction catalyzed by iNOS. A variety of stimuli and inflammatory lesions are associated with accentuated iNOS expression (24). Indeed, the NO produced by iNOS is involved in the generation of reactive nitrogen species which are implicated in tissue lesions. Moreover, NO activates inflammatory signals that exacerbate the inflammatory response. The LPS-exposed cells had elevations in NO and iNOS, relative to untreated cells. However, these increases were reversed in a concentration-dependent fashion by AS treatment. The AS exposure also reduced the levels of pro-inflammatory cytokines in LPS-stimulated RAW264.7 cells, which was consistent with results obtained *in vivo*.

The antioxidant enzymes superoxide dismutase, HO-1 and NAD(P)H oxidoreductase 1 play protective roles against endotoxin-induced inflammation (25). Studies have shown that HO-1 exerts an anti-inflammatory

action under inflammatory conditions through control of nuclear factor- κ B activation and production of inflammatory molecules (26). Treatment with antioxidants reverses CS-induced neutrophil influx and airway inflammation by inducing HO-1 (27). It has been reported that antioxidants down-regulate the expressions of inflammatory cytokines and up-regulate the expression of HO-1 in CSE-stimulated macrophages and bronchial epithelial cells. Therefore, HO-1 induction can be used for treating CS-induced airway inflammation. In the present study, it was found that AS administration up-regulated HO-1 expression and activated Nrf2, relative to the CS + LPS group. It also improved HO-1 expression more effectively than that seen in the NC group, suggesting that AS can be used to induce HO-1 in CS-induced airway inflammation.

These results suggest that AS suppresses the inflammatory response, and possesses therapeutic and prophylactic potential in COPD-associated airway inflammatory response. However, the mechanism of drug action is diverse, and whether astaxanthin can show the effect of COPD through this single pathway remains to be further studied. Thus, it can be considered as a potential drug candidate for the effective treatment for COPD.

Acknowledgements

None.

Interest conflict

No competing interest is associated with this study.

Author contributions

Liu Zhiguang designed the research. Liu Nian, Zhang Weidong, Luo Shujuan, Cao Jun, Peng Minlian and Liu Zhiguang performed the cytotoxicity and reversal experiments. Liu Nian performed PCR and Western blot experiments. All authors analyzed the results and took part in preparing the manuscript.

References

- O'Donnell DE, Aaron S, Bourbeau J, Hernandez P, Marciniuk DD, Balter M, et al. Canadian Thoracic Society recommendations for management of chronic obstructive pulmonary disease - 2007 update. *Can Respir J* 2016; 10: 11.
- Russell R, Norcliffe J, Bafadhel M. Chronic obstructive pulmonary disease: management of chronic disease. *Med* 2016; 44: 310-313.
- Pouwels SD, Hesse L, Faiz A, Lubbers J, Bodha PK, Ten Hacken NH, et al. Susceptibility for cigarette smoke-induced DAMP release and DAMP-induced inflammation in COPD. *Am J Physiol Lung Cell Mol Physiol* 2016; 311: 881-892.
- Gerrit J, Katrin K, Jürgen O, Reda A, Schnelle-Kreis J, Zimmermann R, et al. The composition of cigarette smoke determines inflammatory cell recruitment to the lung in COPD mouse models. *Clin Sci* 2014; 126: 207-221.
- Marwick JA, Kirkham PA, Stevenson CS, Danahay H, Giddings J, Butler K, et al. Cigarette smoke alters chromatin remodeling and induces proinflammatory genes in rat lungs. *Am J Respir Cell Mol Biol* 2004; 31: 633-642.
- Peralta JG, Barnard ML, Turrens JF. Characteristics of neutrophil influx in rat lungs following fecal peritonitis. *Inflammation* 1993; 17: 263-271.
- Cavarra E, Martorana PA, De SM, Bartalesi B, Cortese S, Gambelli F, et al. Neutrophil influx into the lungs of beige mice is followed by elastolytic damage and emphysema. *Am J Respir Cell Mol Biol* 1999; 20: 264-269.
- Gordon S, Martinez FO. Alternative Activation of Macrophages: Mechanism and Functions. *Immunity* 2010; 32: 593-604.
- Bai X, Chen Y, Chen W, Lei H, Gao F, Qin Y, et al. The effect of black coral extraction on acute lung inflammation induced by cigarette smoke in mice. *Exp Lung Res* 2011; 37: 627-632.
- Miravittles M, Soler-Cataluña JJ, Calle M, Soriano JB. Treatment of COPD by clinical phenotypes: putting old evidence into clinical practice. *Eur Respir J* 2013; 41: 1252-1256.
- Bernardo I, Bozinovski S, Vlahos R. Targeting oxidant-dependent mechanisms for the treatment of COPD and its comorbidities. *Pharmacol Ther* 2015; 155: 60-79.
- Guerin M, Huntley ME, Olaizola M. Haematococcus astaxanthin: applications for human health and nutrition. *Trends Biotechnol* 2003; 21: 210-216.
- Pashkow FJ, Watumull DG, Campbell CL. Astaxanthin: a novel potential treatment for oxidative stress and inflammation in cardiovascular disease. *Am J Cardiol* 2008; 101: 58-68.
- Hussein G, Goto H, Oda S, Sankawa U, Matsumoto K, Watanabe H. Antihypertensive potential and mechanism of action of astaxanthin: III. Antioxidant and histopathological effects in spontaneously hypertensive rats. *Biol Pharm Bull* 2006; 29: 684-688.
- Lee JW, Park JW, Shin NR, Park SY, Kwon OK, Park HA, et al. *Picrasma quassiodes* (D. Don) Benn. attenuates lipopolysaccharide (LPS)-induced acute lung injury. *Int J Mol Med* 2016; 38: 834.
- Shin IS, Park JW, Shin NR, Jeon CM, Kwon OK, Lee MY, et al. Melatonin inhibits MUC5AC production via suppression of MAPK signaling in human airway epithelial cells. *J Pineal Res* 2014; 56: 398-407.
- Ham YM, Yoon WJ, Park SY, Song G, Jung YH, Jeon YJ, et al. Quercitrin protects against oxidative stress-induced injury in lung fibroblast cells via up-regulation of Bcl-xL. *J Funct Foods* 2012; 4: 253-262.
- O'Donnell R, Breen D, Wilson S, Djukanovic R. Inflammatory cells in the airways in COPD. *Thorax* 2006; 61: 448.
- Hoenderdos K, Condliffe A. The neutrophil in chronic obstructive pulmonary disease. *American Am J Respir Cell Mol Biol* 2013; 48: 531-539.
- Yadav UCS, Ramana KV, Srivastava SK. Aldose reductase inhibition suppresses airway inflammation. *Chem Biol Interact* 2011; 191: 339-345.
- Stämpfli MR, Anderson GP. How cigarette smoke skews immune responses to promote infection, lung disease and cancer. *Nat Rev Immunol* 2009; 9: 377-384.
- Onizawa S, Aoshiba K, Kajita M, Miyamoto Y, Nagai A. Platinum nanoparticle antioxidants inhibit pulmonary inflammation in mice exposed to cigarette smoke. *Pulm Pharmacol Ther* 2009; 22: 340-349.
- Hsu CL, Fang SC, Huang HW, Yen GC. Anti-inflammatory effects of triterpenes and steroid compounds isolated from the stem bark of *Hiptage benghalensis*. *J Funct Foods* 2015; 12: 420-427.
- Zhang H, Wu MY, Guo DJ, Chanet SW, Lau CC, Chan CO, et al. Gui-ling-gao (turtle jelly), a traditional Chinese functional food, exerts anti-inflammatory effects by inhibiting iNOS and pro-inflammatory cytokine expressions in splenocytes isolated from BALB/c mice. *J Funct Foods* 2013; 5: 625-632.
- Wu X, Song M, Rakariyatham K, Zheng J, Guo S, Tang Z, et al. Anti-inflammatory effects of 4'-demethylnobiletin, a major metabolite of nobiletin. *J Funct Foods* 2015; 19: 278-287.
- Li RJ, Gao CY, Guo C, Zhou MM, Luo J, Kong LY. The Anti-inflammatory Activities of Two Major Withanolides from *Physalis minima* Via Acting on NF- κ B, STAT3, and HO-1 in LPS-Stimulated

RAW264.7 Cells. *Inflammation* 2016; 40: 1-13.

27. Lee JW, Park HA, Kwon OK, Jang YG, Kim JY, Choi BK, et al.

Asiatic acid inhibits pulmonary inflammation induced by cigarette smoke. *Int Immunopharmacol* 2016; 39: 208-217.